Exact analytical solution to ultrasonic interfacial reflection enabling optimal oil film thickness measurement

Min Yu[a✉], Li Shen[a], Tapiwa Mutasa[b], Pan Dou[c], Tonghai Wu[c], Tom Reddyhoff[a]

[a] Department of Mechanical Engineering, Imperial College London, SW7 2AZ, London, United Kingdom

[b] Tribosonics Ltd, S2 4ED, Sheffield, United Kingdom

[c] School of Mechanical Engineering, Xi'an Jiaotong University, 710049, Xi'an, China

✉Corresponding author: m.yu14@imperial.ac.uk

Abstract

The ultrasonic reflection from a lubricated interface has been widely analyzed to measure fluid film thickness, with different algorithms being applied to overcome measurement accuracy and resolution issues. Existing algorithms use either the amplitude or the phase angle of the ultrasonic interfacial reflection. In this paper, a new algorithm (named the "exact model – complex") that simultaneously utilizes both the amplitude and the phase of the complex ultrasonic reflection coefficient is proposed and mathematically derived. General procedures for theoretical analysis in terms of measurement accuracy and uncertainty are proposed and applied to the new algorithm, the beneficial features of which (as compared to other existing algorithms) can be summarized as: 1) a direct calculation, instead of an iterative approximation, 2) guaranteed maximum measurement accuracy, and 3) acceptable measurement uncertainty. None of the existing methods have showed this combination of benefits. Moreover, two groups of raw data from previous experimental studies are utilized to further validate the practical feasibility of the new algorithm. Overall, the proposed "exact model – complex" algorithm fully exploits the potential of ultrasonic reflection for oil film thickness measurement, with an accurate and a convenient calculation suited to practical implementation.

Keywords: film thickness, ultrasonic reflection, complex value, measurement accuracy, measurement uncertainty.

Symbol

c_0	acoustic speed in the film layer in the sandwich structure
c_1	acoustic speed in the layer 1 in the sandwich structure
c_2	acoustic speed in the layer 2 in the sandwich structure
f	signal frequency of the ultrasonic wave
f_c	central frequency of an ultrasonic transducer
f_r	resonant frequency of the exact model
h	actual value of the oil film thickness
$\hat{h}$	calculated value of the oil film thickness with ultrasonic techniques
K	stiffness of the oil film
R_{01}	ultrasonic reflection coefficient at the interface 1 (oil – layer 1) in the sandwich structure
R_{20}	ultrasonic reflection coefficient at the interface 2 (layer 2 – oil) in the sandwich structure
R_a	roughness of the metal surface
R_e	ultrasonic reflection coefficient of the exact model
R_s	ultrasonic reflection coefficient of the spring model
z_0	acoustic impedance of the film layer in the sandwich structure
z_1	acoustic impedance of the layer 1 in the sandwich structure
z_2	acoustic impedance of the layer 2 in the sandwich structure
ρ_0	material density of the film layer in the sandwich structure
ρ_1	material density of the layer 1 in the sandwich structure
ρ_2	material density of the layer 2 in the sandwich structure
$\lvert R_e \rvert$	amplitude of the ultrasonic reflection coefficient
Φ_{R_e}	phase angle of the ultrasonic reflection coefficient

1. Introduction

The oil film thickness is a critical tribological variable that characterises lubrication behaviour. Too thin a lubricant film between sliding components indicates surface contact and wear, while too thick a film can indicate needless viscous dissipation [1]. The measurement of oil film thickness is important in aiding performance tests for formulated lubricants, optimization of surface texture for friction reduction, the development of engine speed control strategies for fuel economy improvement, the health monitoring and fault diagnose for lubricants as well as mechanical components, and so on. In the past decades, three main types of non-invasive liquid lubricant thickness measurement solutions have been developed, including optical techniques (though they are only applicable for transparent materials) [2]-[8], electrical capacitance and resistance (though they may suffer electrical short circuit issues during metal-to-metal asperity contact) [9]-[11], and ultrasonic techniques [12]-[14].

A schematic of the ultrasonic technique applied to oil film thickness measurement is shown in Figure 1, where a pulse is released by an ultrasonic transducer and is incident on a three-layered sandwich structure, with the echo pulse reflected and received by the same transducer. The ratio of the echo pulse to the incident pulse is known as the ultrasonic reflection coefficient, both the amplitude and the phase angle of which are measurable in practice and utilized for the oil film thickness measurement [15]-[17]. Recent research has focused on developing different algorithms that convert the amplitude or the phase angle of the ultrasonic reflection coefficient to the oil film thickness, with the goal of achieving higher measurement accuracy and less measurement uncertainties [18]-[25]. This has been necessary since, until recently, conventional ultrasonic techniques – such as the commonly used "spring model" [15]-[21] have a shortcoming that, for a given transducer frequency range, there is only a limited range of film thicknesses that could be measured. A recent contribution by Dou and co-workers [23], [24] has been important in showing that the range of measurable film thickness values could be significantly increased if the phase of the exact reflection coefficient model is analysed. However, this method has the drawback of requiring an iterative solution (no closed form equation) and also it does not exploit all the available date in the complex reflection coefficient signal.

In this paper, a new algorithm, named the "exact model – complex", is proposed and mathematically derived, enabling: i) a direct calculation (instead of an iterative approximation), ii) guaranteed maximum measurement accuracy over the broadest range of film thickness, and iii) acceptable measurement uncertainty with the ultrasonic central frequency properly selected. The rest of this paper is organized as follows: Section 2 reviews two classical models (the exact model and the spring model) that mathematically describe the relationship between the oil film thickness and the ultrasonic reflection coefficient. Based on the characteristics of these two models, existing algorithms for the oil film thickness calculation are introduced; Section 3 derives a new algorithm for obtaining film thickness with both the amplitude and the phase angle of the ultrasonic reflection coefficient employed simultaneously. General procedures for theoretical

assessment on the measurement accuracy and uncertainty are proposed, with a comprehensive comparison between the proposed and the existing algorithms performed; two groups of raw data from previous experimental tests are utilized in Section 4 to further validate the practical viability of the proposed algorithm, and conclusions are drawn in Section 5.

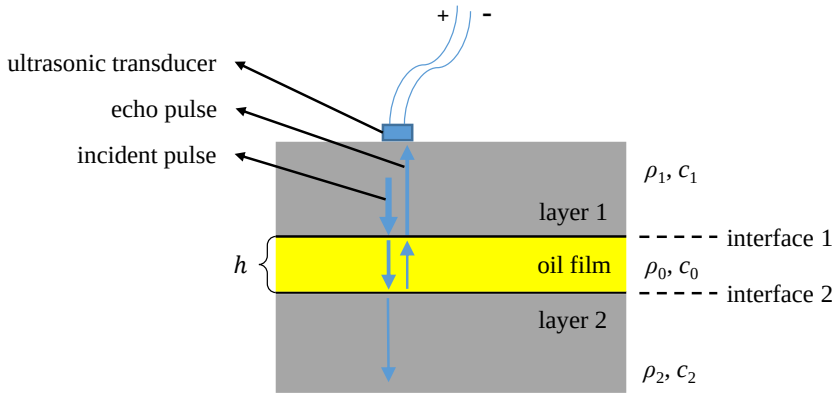

Figure 1 Schematics of an ultrasonic wave travelling through a three-layered sandwich structure.

2. Review of ultrasonic models and measurement algorithms

This section reviews two classical models of the ultrasonic reflection coefficients in a three-layered sandwich structure: the exact model and the linearized spring model. Based on the changes in the amplitude or the phase angle of the ultrasonic reflection coefficient, a group of existing algorithms that calculate the oil film thickness are introduced.

2.1 Exact model of ultrasonic reflection coefficient

An ultrasonic wave travelling through a three-layered sandwich structure is illustrated in Figure 1, where the incident pulse partially transmits through the interface 1, with the rest reflected back, due to the acoustic impedance mismatch between the layer 1 and the oil film. The same phenomenon occurs at the interface 2. The echo pulse is in effect an addition of multiple reflected waves, and the ultrasonic reflection coefficient (*i.e.*, the ratio of the echo pulse to the incident pulse) in a three-layered sandwich structure can be mathematically expressed as below, which is known as the "exact model" [12], [13]:

$$R_e = -\frac{R_{01} + R_{20} \cdot e^{\left(-2\pi f i \cdot \frac{2h}{c_0}\right)}}{1 + R_{01} \cdot R_{20} \cdot e^{\left(-2\pi f i \cdot \frac{2h}{c_0}\right)}} \tag{1}$$

where h is the oil film thickness, f is the frequency of the ultrasonic incident pulse, $R_{01} = \frac{z_0 - z_1}{z_0 + z_1}$ and $R_{20} = \frac{z_2 - z_0}{z_2 + z_0}$ are the reflection coefficients at the interfaces of "oil – layer 1" and "layer 2 – oil" respectively, z_0, z_1 and z_2 correspond to the acoustic impedances of the oil, layer 1 and layer 2, and given as:

$$z_0 = \rho_0 c_0, z_1 = \rho_1 c_1, z_2 = \rho_2 c_2 \tag{2}$$

where ρ_0, ρ_1 and ρ_2 are the density of different materials, and c_0, c_1 and c_2 are the acoustic speed in different materials.

If $z_1 = z_2$, then equation (1) is written as:

$$R_e = -R_{01} \frac{1 - e^{\left(-2\pi f i \cdot \frac{2h}{c_0}\right)}}{1 - {R_{01}}^2 \cdot e^{\left(-2\pi f i \cdot \frac{2h}{c_0}\right)}} \tag{3}$$

If the reflection coefficient is known, the oil film thickness can be calculated by either the amplitude, $|R_e|$,

$$|R_e| = \sqrt{\frac{2{R_{01}}^2 \left[1 - \cos\left(\frac{4\pi f h}{c_0}\right)\right]}{\left(1 + {R_{01}}^4\right) - 2{R_{01}}^2 \cdot \cos\left(\frac{4\pi f h}{c_0}\right)}} \tag{4}$$

or the phase angle, Φ_{R_e},

$$\Phi_{R_e} = \operatorname{atan}\left[\frac{\left(1 - {R_{01}}^2\right)\sin\left(\frac{4\pi f h}{c_0}\right)}{\left(1 + {R_{01}}^2\right)\left(1 - \cos\left(\frac{4\pi f h}{c_0}\right)\right)}\right] \tag{5}$$

It is worth noting that the oil film thickness (h) cannot be obtained directly from equation (4) or (5), and is normally ascertained by numerical iteration and approximation [23]. To enable direct calculation, the exact model is linearized and simplified as follows.

2.2 Spring model of ultrasonic reflection coefficient

Applying the Taylor expansion to the exponential items in (1) and omitting the high-order Taylor items, a linear form of the reflection coefficient, R_s, can be derived and it is commonly referred to as the "spring model" [14]-[15].

$$R_e \approx R_s = \frac{(z_1 - z_2) + \frac{z_1 z_2}{K} \cdot 2\pi f i}{(z_1 + z_2) + \frac{z_1 z_2}{K} \cdot 2\pi f i} \tag{6}$$

where K $(= \frac{\rho_0 c_0^2}{h})$ is denoted as the oil film stiffness.

If $z_1 = z_2$, then equation (6) is further simplified as:

$$R_s = \frac{\frac{z_1}{K} \cdot \pi f i}{1 + \frac{z_1}{K} \cdot \pi f i} = \frac{\left(\frac{z_1}{K} \cdot \pi f\right)^2 + \frac{z_1}{K} \cdot \pi f i}{1 + \left(\frac{z_1}{K} \cdot \pi f\right)^2} \tag{7}$$

The oil film thickness in the spring model can be expressed with respect to the amplitude of the reflection coefficient, $|R_s|$,

$$\hat{h} = h_3(|R_s|) = \frac{\rho_0 c_0^2}{\pi f z_1} \sqrt{\frac{|R_s|^2}{1 - |R_s|^2}} \tag{8}$$

or with respect to the phase angle of the reflection coefficient, Φ_{R_s},

$$\hat{h} = h_4(\Phi_{R_s}) = \frac{\rho_0 c_0^2}{\pi f z_1} \cdot \frac{1}{\tan \Phi_{R_s}} \tag{9}$$

The variation of the amplitude and the phase angle of the reflection coefficient with respect to "frequency × thickness" ($f \cdot h$) are plotted in Figure 2, where both layer 1 and layer 2 are assumed to be steel with the material properties corresponding to Table I. It can be seen the spring model is identical with the exact model when $f \cdot h \ll c_0$, however, both the amplitude ($|R_s|$) and the phase angle (Φ_{R_s}) of the spring model saturate at constant values when $f \cdot h > 0.1 \cdot c_0$. In contrast, the amplitude ($|R_e|$) and the phase angle (Φ_{R_e}) of the exact model show periodic variation, with the first resonance occurring at $f \cdot h = 0.5 \cdot c_0$, which is a beneficial phenomenon for oil film thickness measurement due to the high measurement resolution. Based on these characteristics, a group of existing algorithms, which have different suitable ranges of $f \cdot h$, have been reported to calculate the oil film thickness (h) [19]-[24], as introduced in the following subsection.

Table I Properties of different materials in three-layered structures

Material	Density (kg·m^{-3})	Acoustic speed (m·s^{-1})	Acoustic impedance (10^6 kg·m^{-2}·s^{-1})
oil	941	1461	1.37
steel	7810	5818	45.4
glass	2500	4540	11.4

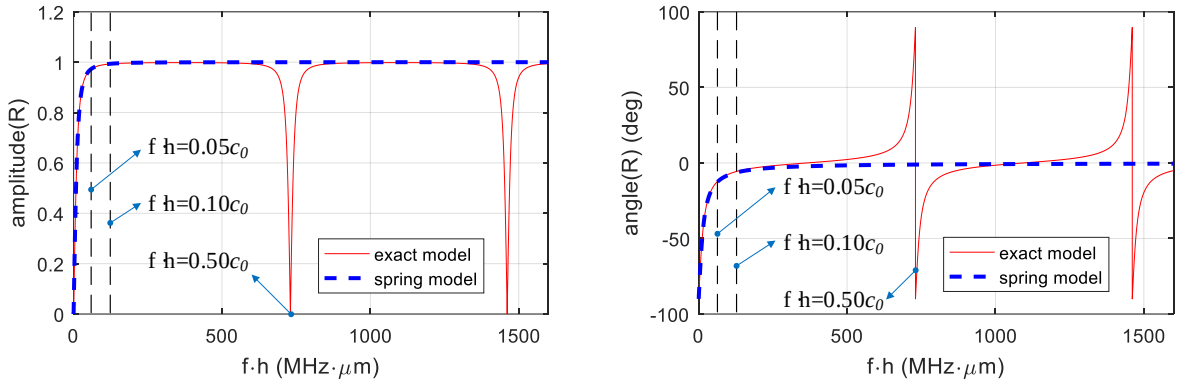

Figure 2 Variation of the amplitude (left) and the phase angle (right) against "frequency × thickness (MHz × μm)" in the exact model and the spring model.

2.3 Existing algorithms for oil film thickness measurement

The measurable amplitude or phase angle of the ultrasonic reflection coefficient is employed to calculate the oil film thickness. Different algorithms have been put forward, and are implemented in practice depending on measurement resolution and accuracy requirements. They are categorized as follows.

1) "exact model – amplitude" [23], [24]: $\hat{h} = h_1(|R_e|)$, see equation (4);
2) "exact model – phase" [23], [24]: $\hat{h} = h_2(\Phi_{R_e})$, see equation (5);
3) "spring model - amplitude" [15]-[17], [21]: $\hat{h} = h_3(|R_s|)$, see equation (8);
4) "spring model – phase" [19]: $\hat{h} = h_4(\Phi_{R_s})$, see equation (9);

The measurement resolution of the above four algorithms is high when $f \cdot h < 0.05 \cdot c_0$, however it is difficult to distinguish changes in the amplitude or the phase angle when $f \cdot h \in [0.1 \cdot c_0, 0.4 \cdot c_0]$, as indicated in Figure 2. Additionally, the algorithms of "spring model – amplitude" and "spring model – phase" may result in notable measurement error when $f \cdot h > 0.05 \cdot c_0$, where the linearized spring model has a significant discrepancy as compared to the exact model. The algorithms of the "exact model – amplitude" and "exact model – phase" require numerical iteration and approximation to obtain the oil film thickness ($\hat{h}$), and thereby it makes the measurement less convenient.

5) "resonance algorithm": amplitude minima/phase zero crossing [14], [23]

When $f \cdot h = 0.5 \cdot n \cdot c_0$, $(n = 1, 2, 3, \ldots)$, both "amplitude minima" and "phase zero crossing" occur, as shown in Figure 2, these phenomena can be utilized to find the corresponding oil film thickness. With the identified first resonant frequency f_r, the oil film thickness is obtained as:

$$\hat{h} = h_5(f_r) = \frac{c_0}{2 \cdot f_r} \tag{10}$$

This algorithm is with the least measurement uncertainty, due to the significant changes in both the measured amplitude and phase angle at around the resonant frequency. However, the

resonance algorithm is only applicable when $f \cdot h > 0.5 \cdot c_0$ (*i.e.*, even for a high frequency transducer of 10 MHz, it is only possible to measure films thicker than 73 μm).

3. Proposed algorithm of "exact model – complex"

To enable a direct calculation and ensure the measurement accuracy (in the non-resonant range of $f \cdot h < 0.5 \cdot c_0$), a new algorithm that simultaneously employs the amplitude and the phase angle of the reflection coefficient in the exact model is proposed to calculate the oil film thickness.

$$\hat{h} = h_6\left(|R_e|, \Phi_{R_e}\right) \tag{11}$$

The proposed algorithm is denoted as "exact model – complex", and it is mathematically derived as follows.

3.1 Mathematical derivation

The complex value of the exact model of the ultrasonic reflection coefficient, R_e, in Euler's notation is:

$$R_e = |R_e| \cdot e^{i \cdot \Phi_{R_e}} = -\frac{R_{01} + R_{20} \cdot e^{-2\pi f i \frac{2h}{c_0}}}{1 + R_{01} \cdot R_{20} \cdot e^{-2\pi f i \frac{2h}{c_0}}} \tag{12}$$

It can be rearranged and given as:

$$e^{-2\pi f i \frac{2h}{c_0}} = \frac{-R_e - R_{01}}{R_{20}(1 + R_e R_{01})} \tag{13}$$

Taking *log* on both sides, yields,

$$2\pi f \frac{2h}{c_0} = i \cdot \ln\left(\frac{-R_e - R_{01}}{R_{20}(1 + R_e R_{01})}\right) \tag{14}$$

If the amplitude and the phase angle of the item $\frac{-R_e - R_{01}}{R_{20}(1+R_e R_{01})}$ are assumed to be r and θ respectively, then,

$$2\pi f \frac{2h}{c_0} = i \cdot \ln\left(r e^{i\theta}\right) = i \cdot \ln(r) - \theta \tag{15}$$

As the item $2\pi f \frac{2h}{c_0} \in \mathbb{R}$, thus $r = 1$ and yields,

$$2\pi f\frac{2h}{c_0} = -\theta = -\operatorname{atan}\left(\frac{-R_e - R_{01}}{R_{20}(1+R_eR_{01})}\right) = -\operatorname{atan}\left(\frac{-|R_e|\cdot e^{i\cdot\Phi_{R_e}} - R_{01}}{R_{20}\left(1+R_{01}\cdot|R_e|\cdot e^{i\cdot\Phi_{R_e}}\right)}\right) \tag{16}$$

Therefore, the oil film thickness h is finally given as a function with respect to $|R_e|$ and Φ_{R_e},

$$\hat{h} = h_6\left(|R_e|,\Phi_{R_e}\right) = \frac{c_0}{4\pi f}\arg\left(\frac{|R_e|\cdot e^{i\cdot\Phi_{R_e}} + R_{01}}{R_{20}\left(1+R_{01}\cdot|R_e|\cdot e^{i\cdot\Phi_{R_e}}\right)}\right) = \frac{c_0}{4\pi f}\operatorname{atan}\left(\frac{|R_e|\cdot\sin\left(\Phi_{R_e}\right)\cdot\left(1-R_{01}^2\right)}{R_{01}+|R_e|^2\cdot R_{01}+|R_e|\cdot\cos\left(\Phi_{R_e}\right)+|R_e|\cdot\cos\left(\Phi_{R_e}\right)\cdot R_{01}^2}\right) \tag{17}$$

where $R_{01} = \frac{z_0 - z_1}{z_0 + z_1}$ and the oil film thickness calculation does not require z_2 (or R_{20}).

This closed form equation calculates film thickness using both the amplitude and phase information of the (measured) reflection coefficient. The proposed algorithm "exact model – complex" is plotted in Figure 3-a), where the results with a group of representative ultrasonic central frequencies f_c = 0.5, 1, 2, and 5 MHz are presented. It can be further interpreted by using the polar coordinate as shown in Figure 3-b), where both the variation of the amplitude $|R_e|$ and the phase angle Φ_{R_e} are utilized to calculate h; in contrast, the algorithm 1) "exact model – amplitude" and 2) "exact model – phase" solely employ the information of $|R_e|$ (*i.e.*, the radius value in polar form) and Φ_{R_e} (*i.e.*, the angular value in the polar coordinate) respectively.

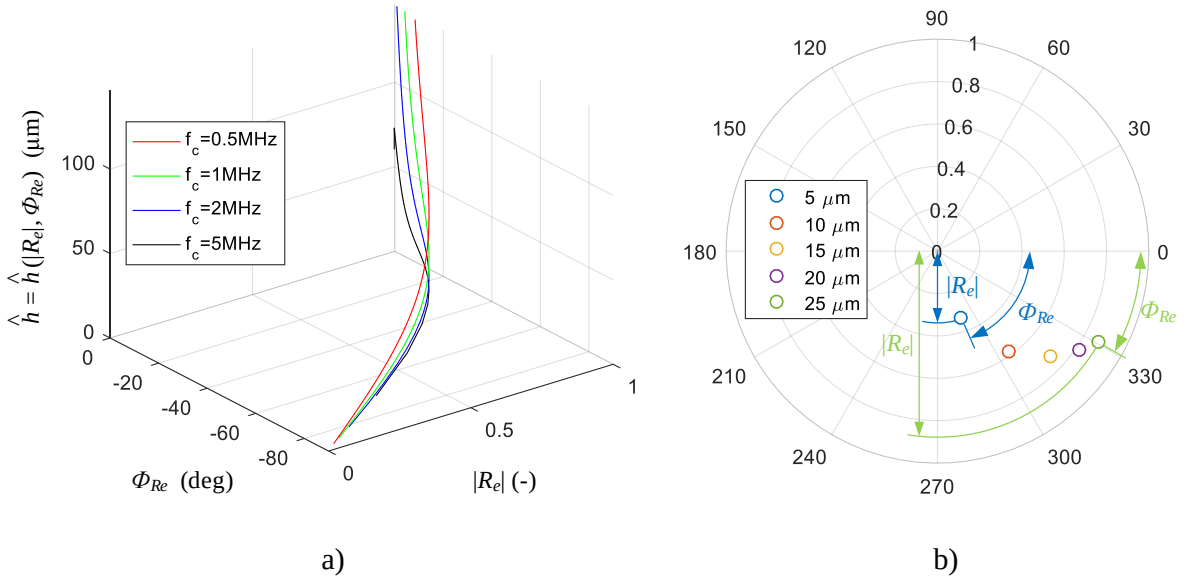

a) b)

Figure 3 a) Proposed algorithm "exact model - complex" in Cartesian coordinates: the calculated oil film thickness ($\hat{h}$) with respect to the two measurable variables of amplitude ($|R_e|$) and the phase angle (Φ_{R_e}). A group of ultrasonic transducers are utilized separately, with the central frequency f_c swept from 0.5 to 1, 2 and 5 MHz; b) location of the complex value R_e with respect to the oil film thickness ($h = [5, 10, 15, 20, 25]\ \mu m$) in polar coordinates. The central frequency of the ultrasonic transducer f_c = 1MHz.

A detailed assessment on both the measurement accuracy and the measurement resolution, together with a comparison to other existing algorithms, are performed in the following subsections. The investigations are only for the non-resonant range of $f \cdot h < 0.5 \cdot c_0$, as the resonance algorithm (amplitude minima/phase angle zero crossing) always has the priority to be employed when $f \cdot h > 0.5 \cdot c_0$.

3.2 Theoretical assessment on measurement accuracy

The procedures for the ultrasonic measurement of the oil film thickness, as well as the assessment on the measurement accuracy, are detailed in Figure 4, where the measurement error (denoted as the final output of "error") is the discrepancy between the calculated and actual values of oil film thickness (*i.e.*, $|\hat{h} - h|$). In practice, the actual value of the oil film thickness in an experimental apparatus can be directly obtained by devices such as a micrometer (as utilized in [23]); however, in the theoretical assessment, the actual value of the oil film thickness used for validation is given by the exact model (as detailed in Section 2.1), which has been proved to be accurate.

The results of the comparison, in terms of theoretical measurement errors between different algorithms, are shown in Figure 5, where the proposed "exact model – complex" is always accurate in the range of $f \cdot h < 0.25 \cdot c_0$, and a constant offset of $0.25 \cdot c_0$ is seen and can be easily compensated when $f \cdot h \in [0.25 \cdot c_0, 0.50 \cdot c_0]$; by contrast, the measurement errors produced by the conventional algorithms "spring model - amplitude" and "spring model – phase" are not negligible when $f \cdot h > 0.05 \cdot c_0$. This suggests that, compared to other methods, the proposed "exact model – complex" enables a widest range of measurable film thicknesses for a given transducer.

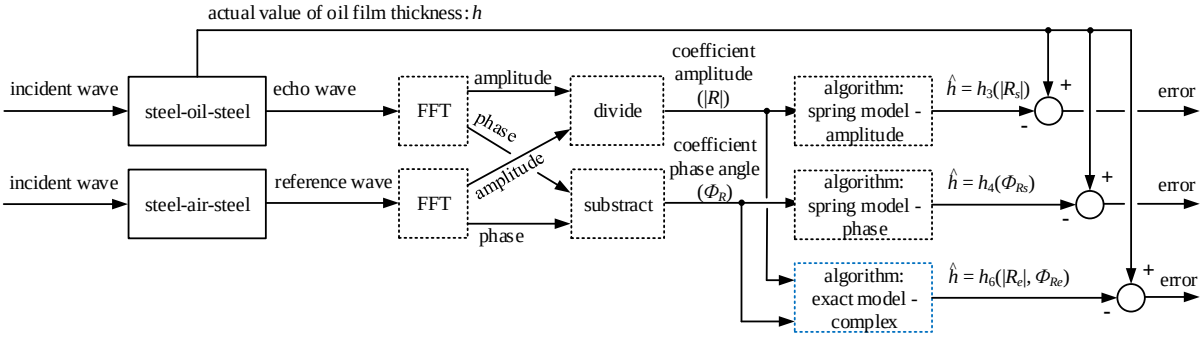

Figure 4 Procedures for the ultrasonic measurement of the oil film thickness and its accuracy assessment. The proposed algorithm "exact model – complex" is highlighted in blue.

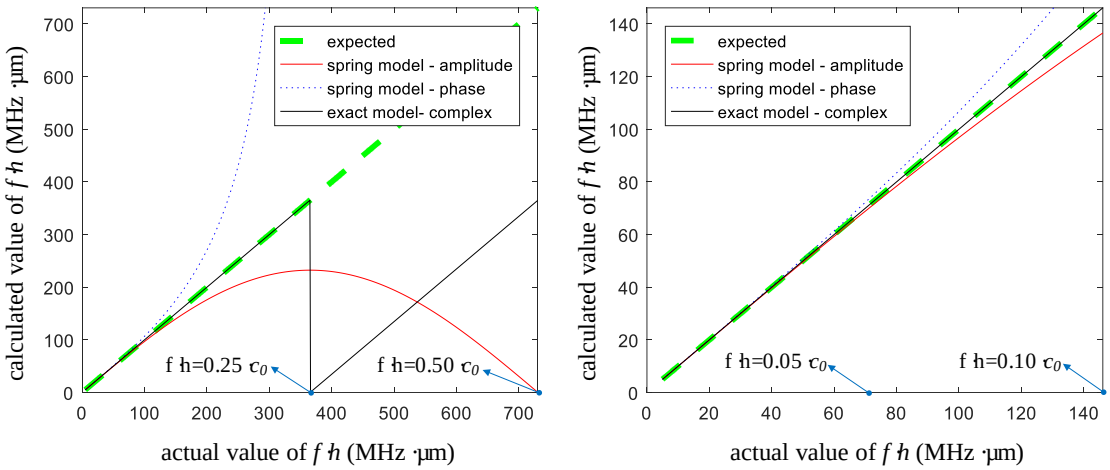

Figure 5 Theoretical analysis of the measurement accuracy with algorithms "spring model – amplitude", "spring model – phase" and proposed "exact model – complex". The left plot shows the discrepancy between the actual and measured values in the range of $f \cdot h < 0.5 \cdot c_0$, and the right one is a zoom-in view of $f \cdot h < 0.1 \cdot c_0$.

3.3 Theoretical assessment on measurement uncertainty

The measurement uncertainty with respect to the oil film thickness (h) has been a critical concern for the ultrasonic technique, as changes in amplitude ($|R_e|$) or phase angle (Φ_{R_e}) are insignificant when $f \cdot h > 0.05 \cdot c_0$. Different algorithms including 1) "exact model – amplitude", 2) "exact model – phase", 3) "spring model - amplitude", 4) "spring model – phase" have been employed or even alternated at different ranges of $f \cdot h$ to improve the measurement resolution [20]-[24]. Furthermore, the ultrasonic central frequency (f_c) also needs to be properly selected.

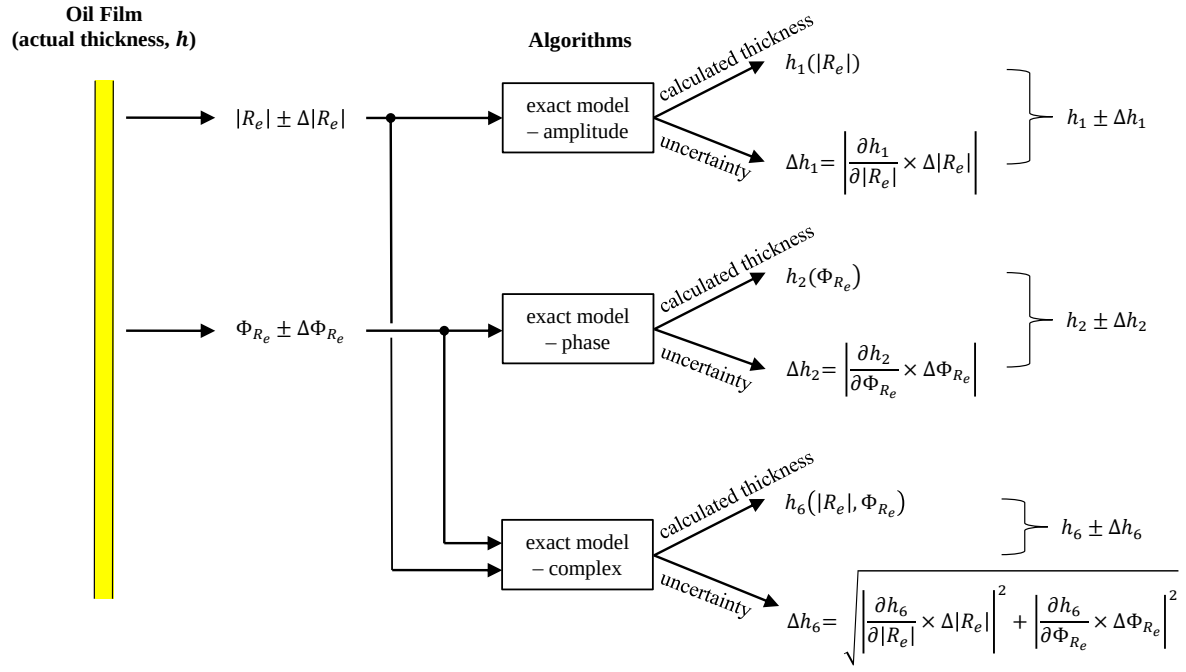

Figure 6 Schematics of measurement uncertainty assessment procedures, with algorithms "exact model – spring", "exact model – phase" and "exact model – complex" compared ($h = h_1 = h_2 = h_6$, according to accuracy analysis).

The schematics of measurement uncertainty assessment procedures with different algorithms are shown in Figure 6, where the calculated thickness results $h_1(|R_e|)$, $h_2(\Phi_{R_e})$ and $h_6(|R_e|, \Phi_{R_s})$ correspond to equations (4), (5) and (17) respectively; and the uncertainty results Δh_1, Δh_2, and Δh_6 are detailed as follows. Uncertainty results of the algorithms "spring model – amplitude, $h_3(|R_s|)$" and "spring model – phase, $h_4(\Phi_{R_s})$" are not shown here, as they are respectively identical with "exact model – amplitude" and "exact model – phase" at low values of $f \cdot h$, while have inaccurate measurement results when $f \cdot h$ is large.

Practically, $|R_e|$ and Φ_{R_e} are measured with independent and random uncertainties, denoted as $|R_e| \pm \Delta|R_e|$ and $\Phi_{R_e} \pm \Delta\Phi_{R_e}$ respectively, where $\Delta|R_e|$ is determined by the voltage measurement resolution, while $\Delta\Phi_{R_e}$ is mainly affected by the sampling frequency. According to error propagation principles, the measurement uncertainty of the algorithm "exact model – amplitude" is:

$$\Delta h_1 = \frac{\partial h_1}{\partial |R_e|} \times \Delta|R_e| = \frac{1}{\frac{\partial |R_e|}{\partial h_1}} \times \Delta|R_e| \tag{18}$$

where the item $\frac{\partial |R_e|}{\partial h_1}$ is derived from equation (4) and shown in equation (19).

$$\frac{\partial(|R_e|)}{\partial h_1} = \frac{\frac{4\pi f}{c_0} R_{01}\left({R_{01}}^4 - 2{R_{01}}^2 + 1\right) \sin\left(\frac{4\pi f h}{c_0}\right)}{\sqrt{2}\left(-2{R_{01}}^2 \cos\left(\frac{4\pi f h}{c_0}\right) + {R_{01}}^4 + 1\right)^{\frac{3}{2}} \sqrt{1 - \cos\left(\frac{4\pi f h}{c_0}\right)}} \tag{19}$$

The measurement uncertainty of the algorithm "exact model – phase" is:

$$\Delta h_2 = \frac{\partial h_2}{\partial \Phi_{R_e}} \times \Delta\Phi_{R_e} = \frac{1}{\frac{\partial \Phi_{R_e}}{\partial h_2}} \times \Delta\Phi_{R_e} \tag{20}$$

where the item $\frac{\partial \Phi_{R_e}}{\partial h_2}$ is derived from equation (5) and shown in equation (21).

$$\frac{\partial \Phi_{R_e}}{\partial h_2} = \frac{4\pi f}{c_0} \frac{\frac{\left(1 - {R_{01}}^2\right)\cos\left(\frac{4\pi f h}{c_0}\right)}{\left(1 + {R_{01}}^2\right)\left(1 - \cos\left(\frac{4\pi f h}{c_0}\right)\right)} - \frac{\left(1 - {R_{01}}^2\right)\sin^2\left(\frac{4\pi f h}{c_0}\right)}{\left(1 + {R_{01}}^2\right)\left(1 - \cos\left(\frac{4\pi f h}{c_0}\right)\right)^2}}{\frac{\left(1 - {R_{01}}^2\right)^2 \sin^2\left(\frac{4\pi f h}{c_0}\right)}{\left(1 + {R_{01}}^2\right)^2 \left(1 - \cos\left(\frac{4\pi f h}{c_0}\right)\right)^2} + 1} \tag{21}$$

The measurement uncertainty of the proposed algorithm "exact model – complex" is:

$$\Delta h_6 = \sqrt{\left|\frac{\partial h_6}{\partial |R_e|} \times \Delta |R_e|\right|^2 + \left|\frac{\partial h_6}{\partial \Phi_{R_e}} \times \Delta \Phi_{R_e}\right|^2} \tag{22}$$

where the items $\frac{\partial h_6}{\partial |R_e|}$ and $\frac{\partial h_6}{\partial \Phi_{R_e}}$ are derived from equation (17).

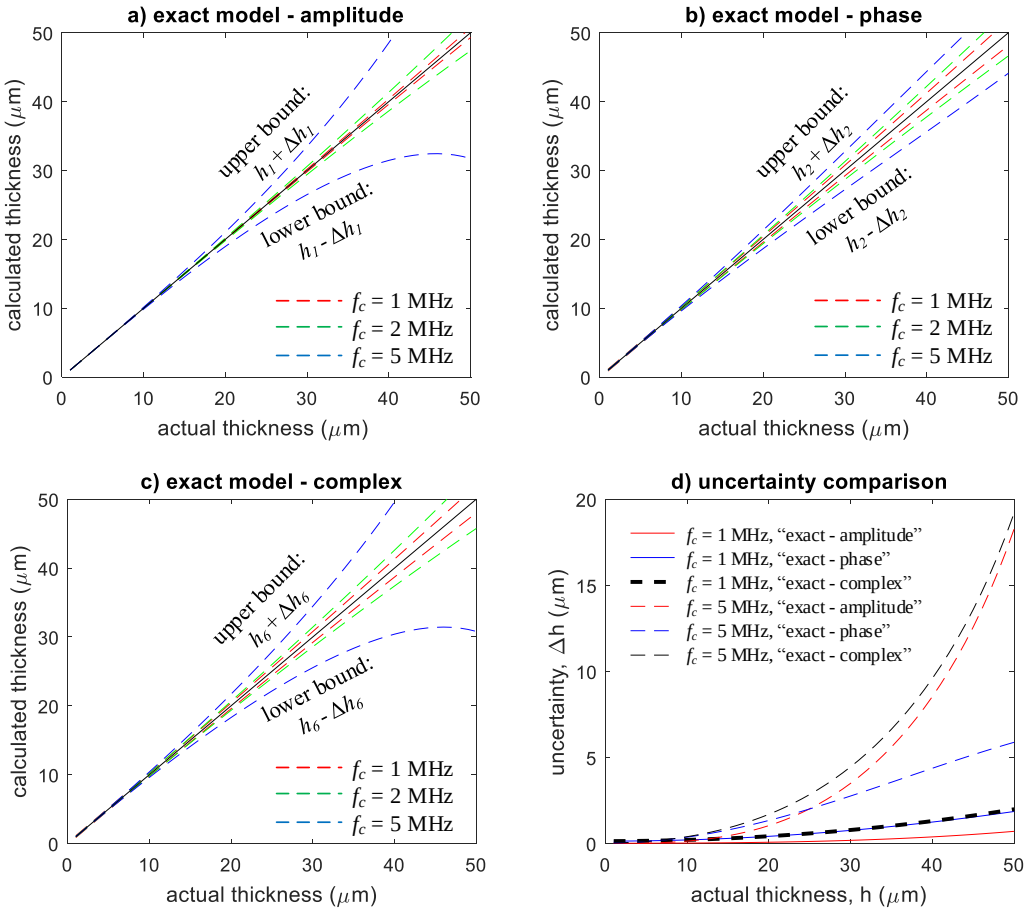

Figure 7 Theoretical analysis of measurement uncertainties: a) "exact model – amplitude", b) "exact model – phase", c) "exact model – complex" and d) comparison between these three algorithms.

Assuming $\Delta|R_e| = 0.1\%$ and $\Delta\Phi_{R_e} = 2\pi \times 0.1\%$, the measurement uncertainties Δh_1, Δh_2 and Δh_6 are plotted in Figure 7-a), b) and c) respectively, where results with the representative ultrasonic frequencies f_c = 1, 2 and 5 MHz are shown. For each algorithm, it can be seen measurement uncertainty (Δh) increases as $f \cdot h$ increases. The algorithm "exact model – amplitude" benefits from with the lowest measurement uncertainty throughout the oil film range $h \in [0, 50]$ μm at the frequency f_c = 1 MHz, while "exact model – phase" has the lowest measurement uncertainty when f_c = 5 MHz. In contrast, the proposed algorithm "exact model – complex" slightly deteriorates the measurement uncertainty compared to other two algorithms, as indicated in Figure 7-d). This is due to the measurement uncertainties in both amplitude and phase being combined, as indicated by the variance formula of error propagation in equation (22). By considering this, an appropriate value of the ultrasonic central frequency needs to be selected

to satisfy both the objective film thickness range and the measurement uncertainty requirement, as detailed in Section 3.4. Overall, the slight deterioration in the measurement uncertainty will not limit the application of proposed algorithm in practical measurements.

3.4 Selection of ultrasonic central frequency

The theoretical analysis in Subsection 3.3 also shows the ultrasonic central frequency (f_c) has significant influence on the measurement uncertainty (or resolution). In practice, since it is not feasible to change the ultrasonic transducer for a different value of f_c, it should be properly selected to obtain decent measurement resolution in the required range of the oil film thickness, $[h_{min}, h_{max}]$.

The resonance algorithm (amplitude minima/phase zero crossing) has priority to be employed due to the guaranteed measurement accuracy and the highest measurement resolution, the central frequency f_c is selected to satisfy the following conditions,

$$\frac{0.5 \cdot c_0}{h_{max}} > (f_c - \Delta f), \frac{0.5 \cdot c_0}{h_{min}} < (f_c + \Delta f) \tag{1}$$

where $[f_c - \Delta f, f_c + \Delta f]$ is known as the frequency bandwidth of an ultrasonic transducer. It can be seen higher frequency transducers lead to the measurement possibility of thinner oil film thickness. However, the signal attenuation cannot be ignored when it is with an extremely high frequency. For example, a 25 MHz ultrasonic wave can only penetrate 10 mm thickness of bearing steel (equivalent to the layer 1 in Figure 1), while 3mm penetration depth for 50 MHz signal transmission [17].

If such an ultrasonic transducer cannot be selected with a feasible value of f_c satisfying the conditions in (1), which is likely to happen for most lubrication systems in the hydrodynamic lubrication regime, then the proposed algorithm "exact model - complex" becomes an alternative solution with f_c properly selected. For example, if the objective film thickness ranges $h \in [0, 50]$ μm and the uncertainty is required as $\Delta h \leq 5$ μm, then the central frequency needs to satisfy $f_c \leq$ 2 MHz, as indicated in Figure 7-c).

All algorithms for the oil film thickness are concluded in Table II, as compared to the conventional algorithms 1)-4), the proposed algorithm "exact model - complex" enables:

- A direct, closed form calculation, instead of requiring iterative approximation (as is the case for the algorithms of "exact model – amplitude" and "exact model – phase", which make the measurement less convenient in practice).
- Guaranteed measurement accuracy (while the algorithms "spring model – amplitude" and "spring model – phase" have notable measurement errors when $f \cdot h > 0.05 \cdot c_0$), as detailed in Subsection 3.2.
- Acceptable measurement uncertainty with an appropriate value of ultrasonic central frequency selected, as shown in Figure 7-c).

Table II Comparison between different algorithms for oil film thickness measurement

Algorithm	Equation	Suitable Range	Direct Calculation
1) Exact model – amplitude [23], [24]	$\hat{h} = h_1(\lvert R_e \rvert)$	$f \cdot h < 0.10c_0$	No
2) Exact model – phase [23], [24]	$\hat{h} = h_2(\Phi_{R_e})$	$f \cdot h < 0.10c_0$	No
3) Spring model – amplitude [15]-[17], [21]	$\hat{h} = h_3(\lvert R_s \rvert)$	$f \cdot h < 0.05c_0$	Yes
4) Spring model – phase [19]	$\hat{h} = h_4(\Phi_{R_s})$	$f \cdot h < 0.05c_0$	Yes
5) Resonance algorithm [14], [23]	$\hat{h} = h_5(f_r)$	$f \cdot h > 0.50c_0$	Yes
6) Exact model – complex	$\hat{h} = h_6(\lvert R_e \rvert, \Phi_{R_e})$	$f \cdot h < 0.10c_0$	Yes

4. Experimental validation

In this section, the raw data from two groups of previous experimental tests, which are with the glass-oil-glass and the steel-oil-steel structures respectively, are utilized here to further validate the practical feasibility of the proposed algorithm "exact model – complex".

4.1 Tests with a three-layered sandwich structure of glass-oil-glass

In an experimental study with the algorithm "spring model – phase", a three-layered structure of "glass-oil-glass" is employed and the utilized ultrasonic transducer has a central frequency of f_c = 2 MHz [19]. The material properties of the glass and the oil correspond to Table I and the oil film thickness varied in the range of $h \in [5, 35]$ μm (the actual value of which is obtained independently by measuring the weight, and dimeter of the sandwiched oil of known density [19]).

The procedures for the ultrasonic measurement of the oil film thickness mainly refer to Figure 4 and are further detailed as follows.

- The oil film in the three-layered sandwich structure is firstly removed, the reflected signal from the "steel-air-steel" structure is then taken as the reference signal.
- A group of the echo signal from the "steel-oil-steel" structure in the time domain is captured, with the oil film thickness swept within $h \in [5, 35]$ μm.
- FFT is performed to both the above reference signal (from the "steel-air-steel" structure) and echo signal (from the "steel-oil-steel" structure) to obtain their representation in the frequency domain.
- The amplitude of the ultrasonic reflection coefficient, $|R_e|$, is the amplitude spectrum of the echo signal (from the "steel-oil-steel" structure) divided by that of the reference signal (from the "steel-air-steel" structure), while the phase spectrum of the echo signal is subtracted by that of the reference signal to yield Φ_{R_e}.

- The oil film thickness is finally calculated by using the proposed algorithm of "exact model – complex", $\hat{h} = h_6(|R_e|, \Phi_{R_e})$ in equation (17).

Figure 8-left shows the raw data of the echo signal (from the "steel-oil-steel" structure) in the time domain, and Figure 8-right gives the final calculated values of the oil film thickness ($\hat{h}$) using the proposed algorithm "exact model – complex". It can be seen the calculated values ($\hat{h}$) essentially correspond to the actual values (h).

Considering the above test conditions of $h \in [5, 35]$ μm and f_c = 2 MHz, which satisfy $f \cdot h < 0.05 \cdot c_0$, all the conventional algorithms ("exact model – amplitude", "exact model – phase", "spring model – amplitude", and "spring model – phase") are applicable and have similar measurement results as those with the proposed "exact model – complex". The proposed "exact model – complex" benefits with a direct calculation, as compared to "exact model – amplitude" and "exact model – phase".

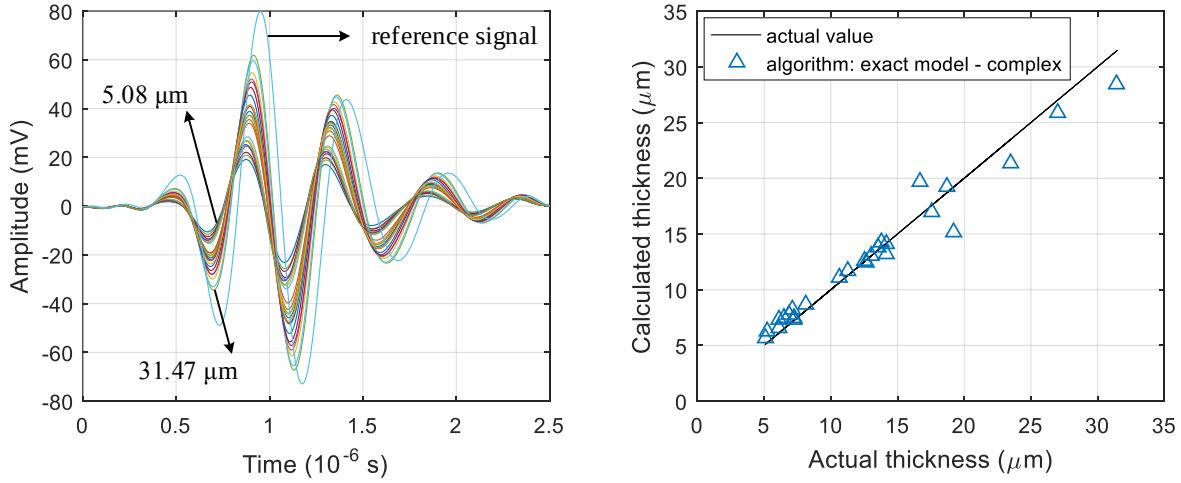

Figure 8 Experimental test results with a three-layered structure of glass-oil-glass: left) the raw data of the echo signal captured in the time domain, with the oil film thickness swept from 5.08 μm to 31.47 μm; right) the calculated value of the oil film thickness ($\hat{h}$) using the algorithm "exact model – complex", as compared the actual value (h).

4.2 Tests with a three-layered sandwich structure of steel-oil-steel

In another experimental study previously performed for the validation of "exact model – phase", a piezo actuator is employed to precisely control the oil film thickness (h) from 4.23 μm to 104.51 μm, and the central frequency of the utilized ultrasonic transducer is f_c = 7 MHz [23]. The raw data is utilized with the same procedures in Subsection 4.1 applied again to assess the proposed algorithm "exact model – complex".

It is worth noting that $h \in [4.23, 61.56]$ μm falls in the non-resonant range and is finally calculated by using the proposed algorithm of "exact model – complex", $\hat{h} = h_6(|R_e|, \Phi_{R_e})$, as given in equation (17). In contrast, $h \in [72.57, 104.51]$ μm is within the resonant range (with the bandwidth of the ultrasonic transducer taken into account), where the "resonance algorithm" (amplitude minima/phase zero crossing), $\hat{h} = h_5(f_r)$, as given in equation (10), can be employed.

The raw data of the echo signal for $h \in [4.23, 61.56]$ μm in the time domain (the reference signal in the dashed line) are presented in Figure 9-left. The final calculated values of the oil film thickness ($\hat{h}$) are compared to the actual values (h), and plotted in Figure 9-right. Despite the variation of different echo waves being "squeezed" and difficult to distinguish, the "exact model – complex" still properly utilizes the phase difference information and shows decent measurement accuracy, as the calculated values ($\hat{h}$) have a good agreement with the actual values (h); whereas a small error ($\hat{h} - h$) is seen when h = 39.14, 50.64, and 61.56 μm, this is due to the increased measurement uncertainty in the range of $f \cdot h \in [0.2 \cdot c_0, 0.3 \cdot c_0]$, as indicated in Subsection 3.3.

Considering the above test conditions of $h \in [4.23, 61.56]$ μm and f_c = 7 MHz, neither the conventional algorithm "spring model – phase" nor "spring model – amplitude" are applicable due to the notable measurement errors ($\hat{h} - h$) in the range of $f \cdot h > 0.05 \cdot c_0$; the algorithm "exact model – phase" has essentially the same measurement results (which are shown in [23]) as "exact model – complex", which benefits direct calculation.

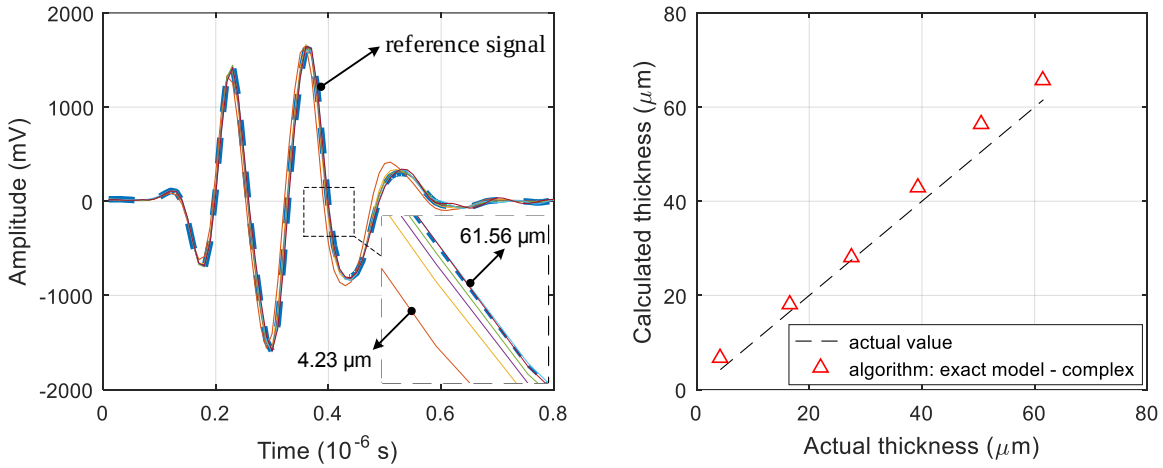

Figure 9 Experimental test results with a three-layered structure of steel-oil-steel: left) the raw data of the echo signal captured in the time domain, with the reference signal in the dashed line and the oil film thickness swept from 4.23 μm to 61.56 μm; right) the calculated value of the oil film thickness ($\hat{h}$) using the algorithm "exact model – complex", as compared to the actual value (h).

5. Conclusions

A new algorithm for the ultrasonic measurement of oil film thickness, named the "exact model – complex", is proposed and mathematically derived in this paper. This consists of a closed form equation (17), which calculates film thickness as a function of both reflection coefficient amplitude and phase. A comprehensive theoretical assessment in terms of the measurement accuracy and the measurement uncertainty is performed to investigate the proposed "exact model – complex", which enables 1) direct calculation, instead of iterative approximation (as is the case for the algorithms of "exact model – amplitude" and "exact model – phase"), 2) guaranteed measurement accuracy, while the algorithms of "spring model – amplitude" and "spring model – phase" have notable measurement errors when $f \cdot h > 0.05 c_0$, and 3) acceptable

measurement uncertainty with an appropriate value of ultrasonic central frequency, despite a slight deterioration is seen as compared to other algorithms.

Moreover, the proposed algorithm is proved to be practically feasible through two groups of experimental results, where the calculated film thickness essentially agrees with the actual value.

Overall, the proposed algorithm “exact model – complex”, together with the existing resonance algorithm (amplitude minima/phase zero crossing), will be able to fully exploit the potential of the ultrasonic technique and to deal with most oil-lubricated systems, with measurement accuracy and calculation convenience provided.

Acknowledgements

The authors are very grateful to Tribosonics for providing useful discussion and expertise.

Reference

[1] Cen, H., & Lugt, P. M. (2019). Film thickness in a grease lubricated ball bearing. *Tribology international*, *134*, 26-35. https://doi.org/10.1016/j.triboint.2019.01.032

[2] Gohar, R., & Cameron, A. (1963). Optical measurement of oil film thickness under elasto-hydrodynamic lubrication. *Nature*, *200*(4905), 458-459. https://doi.org/10.1038/200458b0

[3] Chen, Y., Zhang, X., Zhang, P., & Liu, C. (2009, June). Lubricant film thickness measurement using fiber-optic Michelson interferometer and fiber-optic displacement sensor. In *2009 International Conference on Information and Automation* (pp. 951-956). IEEE. https://doi.org/10.1109/ICINFA.2009.5205055

[4] Dyson, A. H. A. R., Naylor, H., & Wilson, A. R. (1965, June). Paper 10: the measurement of oil-film thickness in elastohydrodynamic contacts. *Proceedings of the Institution of Mechanical Engineers, Conference Proceedings* (Vol. 180, No. 2, pp. 119-134). Sage UK: London, England: SAGE Publications.

[5] Sherrington, I., & Smith, E. H. (1985). Experimental methods for measuring the oil-film thickness between the piston-rings and cylinder-wall of internal combustion engines. *Tribology International*, *18*(6), 315-320. https://doi.org/10.1016/0301-679X(85)90077-5

[6] Vlădescu, S. C., Medina, S., Olver, A. V., Pegg, I. G., & Reddyhoff, T. (2016). Lubricant film thickness and friction force measurements in a laser surface textured reciprocating line contact simulating the piston ring–liner pairing. *Tribology International*, *98*, 317-329. https://doi.org/10.1016/j.triboint.2016.02.026

[7] Marx, N., Guegan, J., & Spikes, H. A. (2016). Elastohydrodynamic film thickness of soft EHL contacts using optical interferometry. *Tribology International*, *99*, 267-277. https://doi.org/10.1016/j.triboint.2016.03.020

[8] Ford, R. A. J., & Foord, C. A. (1978). Laser-based fluorescence techniques for measuring thin liquid films. *Wear*, *51*(2), 289-297. https://doi.org/10.1016/0043-1648(78)90267-3

[9] Irani, K., Pekkari, M., & Ångström, H. E. (1997). Oil film thickness measurement in the middle main bearing of a six-cylinder supercharged 9 litre diesel engine using capacitive transducers. *Wear*, *207*(1-2), 29-33. https://doi.org/10.1016/S0043-1648(96)07470-4

[10] Cheng, M. H. M., Chiu, G. T. C., & Franchek, M. A. (2009, June). Real-time measurement of eccentric motion with capacitive sensor for hydraulic pumps. In *2009 American Control Conference* (pp. 3687-3692). IEEE. https://doi.org/10.1109/ACC.2009.5160063

[11] Chao, Q., Zhang, J., Xu, B., & Wang, Q. (2018). Multi-position measurement of oil film thickness within the slipper bearing in axial piston pumps. *Measurement*, *122*, 66-72. https://doi.org/10.1016/j.measurement.2018.03.016

[12] Brekhovskikh, L. (2012). *Waves in layered media* (Vol. 16). Elsevier.

[13] Haines, N. F., Bell, J. C., & McIntyre, P. J. (1978). The application of broadband ultrasonic spectroscopy to the study of layered media. *The Journal of the Acoustical Society of America*, *64*(6), 1645-1651. https://doi.org/10.1121/1.382131

[14] Pialucha, T., & Cawley, P. (1994). The detection of thin embedded layers using normal incidence ultrasound. *Ultrasonics*, *32*(6), 431-440. https://doi.org/10.1016/0041-624X(94)90062-0

[15] Dwyer-Joyce, R. S., Drinkwater, B. W., & Donohoe, C. J. (2003). The measurement of lubricant–film thickness using ultrasound. *Proceedings of the Royal Society of London. Series A: Mathematical, Physical and Engineering Sciences*, *459*(2032), 957-976. https://doi.org/10.1098/rspa.2002.1018

[16] Dwyer-Joyce, R. S., Harper, P., & Drinkwater, B. W. (2004). A method for the measurement of hydrodynamic oil films using ultrasonic reflection. *Tribology Letters*, *17*(2), 337-348. https://doi.org/10.1023/B:TRIL.0000032472.64419.1f

[17] Dwyer-Joyce, R. S., Reddyhoff, T., & Drinkwater, B. W. (2004). Operating limits for acoustic measurement of rolling bearing oil film thickness. *Tribology transactions*, *47*(3), 366-375. https://doi.org/10.1080/05698190490455410

[18] Zhang, J., Drinkwater, B. W., & Dwyer-Joyce, R. S. (2005). Calibration of the ultrasonic lubricant-film thickness measurement technique. *Measurement science and technology*, *16*(9), 1784. https://doi.org/10.1088/0957-0233/16/9/010

[19] Reddyhoff, T., Kasolang, S., Dwyer-Joyce, R. S., & Drinkwater, B. W. (2005). The phase shift of an ultrasonic pulse at an oil layer and determination of film thickness. *Proceedings of the Institution of Mechanical Engineers, Part J: Journal of Engineering Tribology*, *219*(6), 387-400. https://doi.org/10.1243%2F135065005X34044

[20] Reddyhoff, T., Dwyer-Joyce, R., & Harper, P. (2006). Ultrasonic measurement of film thickness in mechanical seals. *Sealing Technology*, *2006*(7), 7-11. https://doi.org/10.1016/S1350-4789(06)71260-0

[21] Reddyhoff, T., Dwyer-Joyce, R. S., & Harper, P. (2008). A new approach for the measurement of film thickness in liquid face seals. *Tribology Transactions*, *51*(2), 140-149. https://doi.org/10.1080/10402000801918080

[22] Mills, R., Vail, J. R., & Dwyer-Joyce, R. (2015). Ultrasound for the non-invasive measurement of internal combustion engine piston ring oil films. *Proceedings of the Institution of Mechanical Engineers, Part J: Journal of Engineering Tribology*, *229*(2), 207-215. https://doi.org/10.1177%2F1350650114552538

[23] Dou, P., Wu, T., & Luo, Z. (2019). Wide range measurement of lubricant film thickness based on ultrasonic reflection coefficient phase spectrum. *Journal of Tribology*, *141*(3), 031702. https://doi.org/10.1115/1.4041511

[24] Zhang, K., Dou, P., Wu, T., Feng, K., & Zhu, Y. (2019). An ultrasonic measurement method for full range of oil film thickness. *Proceedings of the Institution of Mechanical Engineers, Part J: Journal of Engineering Tribology*, *233*(3), 481-489. https://doi.org/10.1177%2F1350650118787038

[25] Kæseler, R. L., & Johansen, P. (2019). Adaptive ultrasound reflectometry for lubrication film thickness measurements. *Measurement Science and Technology*, *31*(2), 025108. https://doi.org/10.1088/1361-6501/ab35f2